Assessment of critical parameters affecting the behaviour of bearing reinforced concrete walls under fire exposure

Abstract

Purpose - This research paper aims to investigate RC walls' behaviour under fire and identify the thermal and mechanical factors that affect their performance.

Design/methodology/approach - A three-dimensional (3-D) finite element (FE) model is developed to predict the response of RC walls under fire, and is validated through experimental tests on RC wall specimens subjected to fire conditions. The numerical model incorporates temperature-dependent properties of the constituent materials. Moreover, the validated model was used in a parametric study to inspect the effect of the fire scenario, reinforcement concrete cover, reinforcement ratio and configuration, and wall thickness on the thermal and structural behaviour of the walls subjected to fire.

Findings - The developed 3-D FE model successfully predicted the response of experimentally tested RC walls under fire conditions. Results showed that the fire resistance of the walls was highly compromised under hydrocarbon fire. In addition, the minimum wall thickness specified by EC2 may not be sufficient to achieve the desired fire resistance under considered fire scenarios.

Originality/value – There is limited research on the performance of RC walls exposed to fire scenarios. The study contributed to the current state-of-the-art research on the behaviour of RC walls of different concrete types exposed to fire loading, and it also identified the factors affecting the fire resistance of RC walls. This guides the consideration and optimisation of design parameters to improve RC walls performance in the event of a fire.

Paper type Research paper

Keywords: normal-strength concrete, high-strength concrete, fire, walls, finite element modelling.

1. Introduction

Reinforced concrete (RC) walls comprise a significant part of most of the existing residential buildings. Since they offer considerable load-bearing capacity for gravity and lateral-force resisting systems, they have been extensively used in tall buildings and high-rise towers. Therefore, RC-bearing walls should provide proper fire resistance to withstand static loads during fire scenarios. Several experimental investigations have been performed on the behaviour of RC walls subjected to fire in the last decades [1]–[9].

One of the earliest attempts was carried out by Crozier and Sanjayan [1] testing 18 full-scale RC walls under one-sided ASTM E119 standard fire exposure. These researchers concluded that the walls reinforced with one mat in the middle of the wall offered better fire resistance than those reinforced at the two sides, which can be attributed to a larger concrete cover and hence, better reinforcement protection. Furthermore, the findings of Mueller's and Kurama's study [2] revealed that inadequate reinforcement near the wall's surfaces results in out-of-plane buckling, leading to a premature failure at a much earlier fire duration. Further parameters affect the response of RC walls under fire, namely, the concrete compressive strength, slenderness ratio, reinforcement ratio, axial load and lateral load levels, and boundary conditions, among others. The effect of concrete compressive strength was extensively studied in the literature. Most of the conducted studies [3]–[5] reported that the increase in concrete compressive strength leads to lower fire resistance and failure in the form of explosive spalling [5]. However, Zheng and Zhuang [6] reported an increase in the fire resistance of RC walls when the concrete compressive strength is higher due to the larger bearing capacity of the walls. Slenderness ratio and/or wall thickness considerably influence the behaviour of RC walls exposed to fire [3]. Chen et al. [7] observed that the fire resistance of RC walls exponentially increases with the increase of wall thickness for all load levels. Mueller and Kurama [8] inspected the effect of boundary conditions on the out-of-plane behaviour of RC walls subjected to one-sided standard fire exposure. They tested two full-scale RC walls where one of the specimens was laterally restrained at the top, and the other was subjected to an increasing lateral force. Larger curvatures, through-thickness cracks, and out-of-plane displacements were documented for the later specimen. The effect of lateral load was studied in other previous investigations [8]–[10]. In general, applying a lateral load in the out-of-plane direction adversely affected the fire resistance of RC walls. Moreover, an induced shear force could take place in the wall due to thermal bowing during the fire, as discussed by Mueller and Kurama [9] and Kumar and Kodur [11]. Few publications examined the in-plane lateral load effect of seismic or wind loading. However, studying the behaviour of RC walls subjected to both in-plane lateral loads and fire loads is crucial to assess their response during an earthquake-induced fire incident.

The push toward performance-based building standards and performance-based fire safety design has been influenced by the expanding usage and widespread acceptance of computer-based analytical methodologies within the fire safety engineering community [12]–[19]. Fire safety engineering lacks a standard framework for assessing analytical techniques with well-known uncertainty bounds. Even though much work has been put into creating a common framework over the last decade, it is not yet comprehensive and integrated. Since experimental testing of reinforced concrete members under fire demands considerable effort and expensive equipment, computational methods are imperative to predict the behaviour of RC structures under fire exposure.

A number of studies opted to model the fire performance of RC walls [7], [20]–[27]. For example, Lee and Lee [24] created a theoretical model that simulates the axial behaviour of experimentally tested RC walls under all-sided fire exposure. Their test results and model predictions showed an initial axial extension of the wall followed by contraction. They also conducted a parametric study on the effects of wall thickness, reinforcement ratio, concrete compressive strength, and axial load level. Chen et al. [28] had similar findings; they modelled RC walls subjected to one-sided fire exposure and found that the most influential factors on the fire resistance of RC walls were the wall thickness and the load level. Their results indicated that concrete compressive strength and reinforcement ratio had minimal effect on the fire resistance of the modelled walls. However, Chen et al. [28] results showed that the wall's fire resistance is linearly affected by the increase or decrease of the wall thickness or reinforcement ratio.

Mueller and Kurama [20] modelled three full-scale RC walls which they tested in previous experimental programs [2], [10]. They simultaneously performed thermo-mechanical sequential analysis using the commercial software SAFIR to simulate the out-of-plane behaviour of the tested walls subjected to one-sided standard fire with axial and lateral loads. They verified the axial and out-of-plane displacements of the modelled walls. Kumar and Kodur [11] numerical study emphasised a similar out-of-plane behaviour of RC walls with the same load scenarios obtained from the numerical simulation performed in ANSYS [29]. No further parametric studies were conducted in either study. Kang et al. [23] analysed fire-damaged RC walls in ABAQUS and evaluated the effect of the axial load and wall thickness on the residual bearing capacity of RC walls. Wall thickness was observed to have a significant impact on the bearing capacity of the walls. Similarly, Ryu et al. [22] inspected the effect of compressive strength and heated areas on the residual strength of the heated walls. These authors did not report any difference in the residual bearing capacity of the walls heated on one side or both sides.

Limited research was conducted on RC walls exposed to fire scenarios other than the ASTM E119 standard fire [30]. One experimental study by Ngo et al. [5] examined the effect of the hydrocarbon fire scenario on the behaviour of normal-strength and high-strength RC walls. The performance of the walls under hydrocarbon fire was compared with those exposed to ASTM E119 standard fire with varying eccentricity and axial loading. Ten large-scale RC walls were tested, of which six walls passed the 2-hour duration of the fire without failure, and the remaining four walls experienced concrete spalling. The failed walls were high-strength concrete walls subjected to hydrocarbon fire. Ngo et al. [5] concluded that the hydrocarbon fire produces far more intense and greater spalling in high-strength concrete walls than a standard fire. Thus, it is important to study the response of structural elements when exposed to different fire scenarios and fire intensities. This is vital when considering the importance of the facility being designed and the extent of the risk it experiences during its lifetime.

This study used advanced numerical modelling to explore the impact of critical parameters that influence the response of RC walls under fire exposure. The investigated parameters are wall thickness, reinforcement ratio and configuration, concrete cover, and fire scenario. Moreover, the parameter investigation results were used to assess some of the design guidelines regarding structural fire resistance in existing codes of practice.

2. Description of the FE numerical model

A three-dimensional (3-D) FE element model was developed in ABAQUS 19 [31] to simulate the behaviour of RC walls under fire exposure. Two types of FE models were created: thermal and structural. Heat transfer analysis was conducted in the thermal model to obtain temperature profiles and nodal temperatures. Then, thermal analysis results were incorporated into the structural model to perform mechanical stress analysis, where stresses and displacements of the wall elements were obtained. The geometry and material properties of the wall specimens were taken from Ngo et al. [5] and Mueller and Kurama [8].

2.1.Geometrical configuration

Three wall specimens were created to simulate the behaviour of experimentally tested walls by Ngo et al. [5] and Mueller and Kurama [8]. The first two specimens had a length of 2400 mm, a width of 1000 mm, and a thickness of 150 mm and were exposed to a two-hour fire load following ASTM E-119 fire curve [5]. The main reinforcement bars had a diameter of 16 mm and were spaced at 300 mm. The walls have a transverse reinforcement of 14 mm hoops at 300 mm spacing. The only difference between the two specimens is the type of concrete. The first specimen (WALL1) was a normal-strength concrete (NSC) wall, and the second specimen (WALL2) was a high-strength concrete (HSC) wall. The third specimen (WALL3) had a length, thickness, and width of 3050, 1020, and 380 mm, respectively, and was exposed to an 8-hour fire load following ASTM E-119 fire curve [8]. It was reinforced with 25 mm diameter bars in the longitudinal direction and 13 mm outer hoops in the transverse direction. Additionally, all middle rebars were tied with 13 mm diameter transverse ties. Table 1 summarises the properties of the reference walls. Fig. 1 illustrates the geometrical configuration and reinforcement of the simulated wall specimens and the developed FE models in ABAQUS. To save computational time, symmetry along the width of the wall was used. Hence, half of the wall was modelled providing roller supports along its height to restrict the movement of the wall in the direction of symmetry. In the mechanical/structural model, the walls were modelled to be simply supported at the bottom and restrained in the axial direction at the top.

Table 1: Summary of the modelled walls properties

Property	***WALL1*** [5]	***WALL2*** [5]	***WALL3*** [8]
Dimensions (mm) (LengthxWidthxThickness)	2400×1000 ×150	2400×1000 ×150	3050×1020 ×380
Longitudinal reinforcement	8Ø16	8Ø16	10Ø25
Horizontal reinforcement	Ø14@300 mm	Ø14@300 mm	Ø13@230 mm
Concrete strength (MPa)	32	60	46
Axial load (kN)	485	970	2400

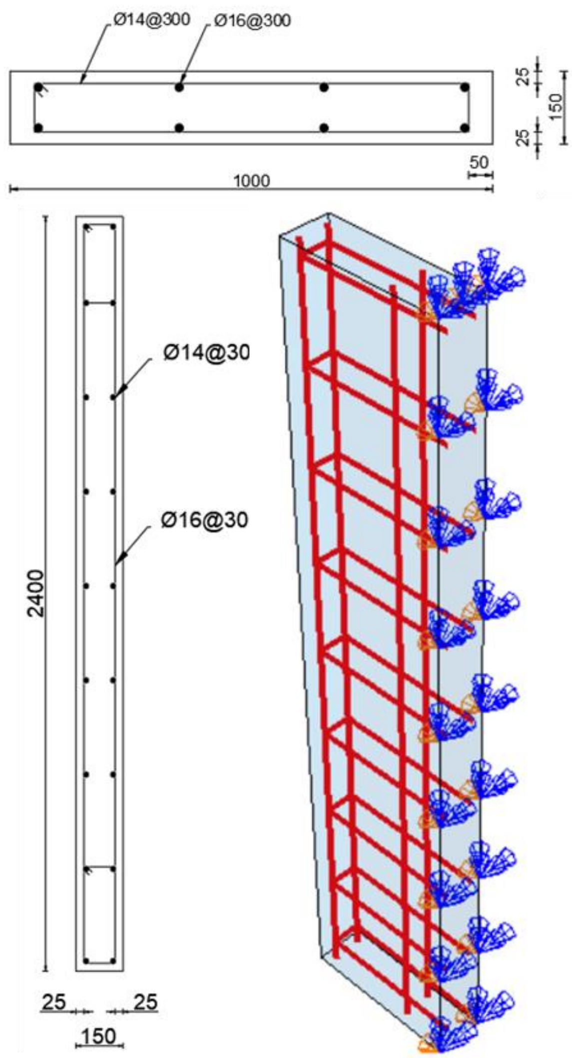

(a)

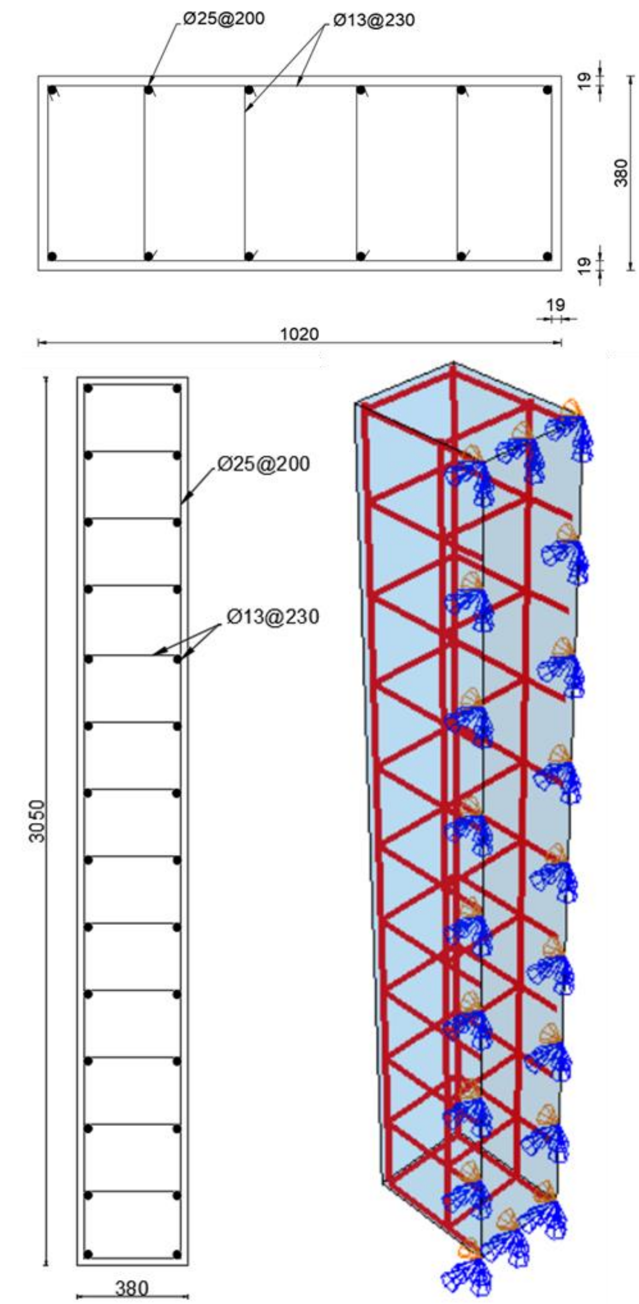

(b)

Fig. 1: Details of the modelled walls and the corresponding developed FE models

2.2. Elements description

Since two types of analyses were conducted in this study (thermal and structural), each analysis process utilised a specific type of elements from the element library within ABAQUS [26]. In the thermal model, concrete is modelled using the DC3D8 element, where DC3 denotes a diffusive heat-transfer, three-dimensional solid element, and D8 represents the 8 degrees of freedom, Fig. 2. Steel reinforcement was modelled using DC1D2, which is a 2-node linear truss element, Fig. 2. Both elements have linear interpolation functions for temperature within the element. Therefore, linear temperature variation between the nodes is assumed. Moreover, the two elements can transfer heat by conduction, convection, and radiation.

The geometrical and mesh configurations are transferred from the thermal model to the structural model. However, concrete and steel reinforcement elements are assigned suitable stress/displacement analysis element types. Concrete was modelled using a C3D8 element, a continuum, three-dimensional solid element with the same layout and number of nodes as the DC3D8 element, and the steel rebars were assigned a C1D2 element, which is identical to the DC1D2 thermal element.

(a) DC3D8 and C3D8 (b) DC1D2 and C1D2

Fig. 2: Representation of used elements in the FE model

2.3. Material properties

Thermal and mechanical properties of concrete and steel reinforcement deteriorate with increasing temperature. Hence, capturing the accurate behaviour of the RC walls under fire requires incorporating the material properties variation with temperature. This section summarises the material models utilised in developing the FE model.

2.3.1 Thermal properties

The material properties required to simulate the thermal behaviour of RC structures under elevated temperatures are thermal conductivity, specific heat, and density of concrete and reinforcing steel, respectively. Thermal material models for normal-strength concrete and steel reinforcement are defined based on the specified provisions in Eurocode (EC2) [32]. However, for high-strength concrete, EC2 permits using applicable developed models for thermal conductivity and specific heat. Thus, material models defined for high-strength concrete in [33] were adopted in this study.

2.3.2 Mechanical properties

The material parameters required for the stress analysis are the elastic modulus, Poisson's ratio, stress-strain curves, thermal elongation, and tensile strength for both concrete and steel reinforcement, and the concrete compressive strength. The variation of these properties with increasing temperatures is crucial in determining the structural behaviour of RC walls under fire exposure. This study adopted the EC2 [27] models for the constituent materials' mechanical properties. Fig. 3 illustrates the compressive strength variation for normal-strength and high-strength concrete. The elastic modulus was calculated as $4700\sqrt{f'_c}$ for all temperature values; therefore, it followed the assumed reduction in the compressive strength. Class 1 reduction factors were taken for high-strength concrete since the compressive strength of concrete in the reference paper is 60 MPa [5]. It should be noted that the compressive strength variation affects concrete's linear and non-linear properties, namely, the elastic modulus and stress-strain curves.

The non-linear properties of concrete and steel reinforcement were incorporated into the FE model. The steel was modelled using a bilinear curve, which exhibits a plateau behaviour where the stress remains roughly constant, and the strain increases after exceeding the yield strength. The Kent and Park [34] constitutive model for unconfined concrete was used to represent the stress-strain curve for concrete in compression. According to Kent and Park [34], the compressive stress (σ_c) is calculated by Eq. (1):

$$\sigma_c = \sigma_{cu}[2\frac{\varepsilon_c}{\varepsilon'_c} - (\frac{\varepsilon_c}{\varepsilon'_c})^2] \quad (1)$$

where σ_{cu} and ε'_c are the ultimate compressive strength and the strain of the unconfined cylinder specimen, respectively. σ_c is the nominal compressive stress corresponding to the strain ε_c.

The tensile behaviour of concrete was approximated using the simplified linear-softening model. In this model, the stress-strain curve of concrete in tension is assumed to be linear up to peak stress, representing the maximum tensile stress that the concrete can withstand before failure. After the peak stress is reached, the material rapidly softens, and the stress drops to zero as the material fails.

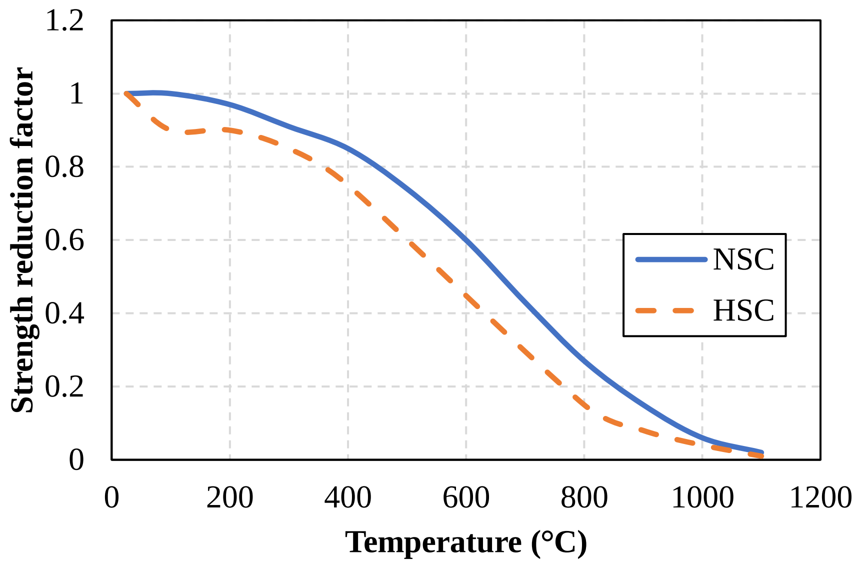

Fig. 3: Strength reduction models of concrete

2.3.2.1 Concrete damage plasticity model

The Concrete Damaged Plasticity (CDP) model in ABAQUS is a material model used to simulate the behaviour of concrete under various loading conditions [35]. The CDP model provides a comprehensive way to simulate the behaviour of concrete under various loading conditions, considering the effects of plasticity, damage, and hardening. It is based on the assumption that the concrete undergoes plastic deformation before failure and that material damage occurs during the process. This model uses an isotropic damage model, meaning that the damage is assumed to be the same in all directions. It consists of three main components: a plasticity model, a damage model, and a hardening model. The plasticity model is based on the Drucker-Prager yield criterion, which assumes the concrete behaves like a frictional material. Moreover, the model considers the effects of stress triaxiality, strain hardening, and strain rate sensitivity. It is also based on the assumption that the concrete undergoes microcracking before macroscopic failure. The model uses a damage parameter that ranges from 0 (no damage) to 1 (complete damage) to represent the level of damage in the material. The damage parameter is updated based on the accumulated strain energy density in the material. Finally, the hardening model considers strain hardening and softening effects on the material. The model assumes that the concrete undergoes strain hardening up to a certain point, after which it begins to undergo strain softening. The softening behaviour is modelled using a stress-strain curve, which is based on the damage parameter.

The CDP model was applied to the concrete's compression and tension behaviour. For compression, damage depends on the inelastic strain hardening, and it was calculated as in Eq. 2. The damage parameter (d_c) was 0 at the maximum compressive stress, decreasing until it reached 0.8 for 20% remaining strength. Similarly, the tension damage increases with the increase in the hardening cracking strain. Therefore, it can be calculated as in Eq. 3.

$$d_c = 1 - \frac{\sigma_c}{\sigma_{cu}} \quad (2)$$

$$d_t = 1 - \frac{\sigma_t}{\sigma_{tu}} \quad (3)$$

Where, σ_{cu} and σ_{tu} are the ultimate compressive and tensile strength of concrete, respectively. σ_c and σ_t the compressive and tensile stress correspond to the inelastic and cracking strains, respectively.

2.4. Heat transfer analysis

Transient heat-transfer analysis was performed in ABAQUS. The time-dependent temperature distribution in the wall is determined by Fourier's equation (4):

$$\frac{\partial}{\partial x}\left(k\frac{\partial T}{\partial x}\right) + \frac{\partial}{\partial y}\left(k\frac{\partial T}{\partial y}\right) + \frac{\partial}{\partial Z}\left(k\frac{\partial T}{\partial Z}\right) = \rho C\frac{\partial T}{\partial t} \quad (4)$$

where: k is the thermal conductivity, ρ is the density, and C is the specific heat. If the heat flux is assumed to be negligible through the x and y directions (length and width), then the equation becomes:

$$\frac{\partial}{\partial z}\left(k\frac{\partial T}{\partial z}\right) = \rho C\frac{\partial T}{\partial t} \qquad (5)$$

Convection and radiation develop due to heat flux exchange with the wall's outermost surfaces. Taking them into account, the governing differential equation becomes:

$$-k\frac{\partial T}{\partial z} = h_c\left(T - T_f\right) + \sigma\varepsilon_m\varepsilon_f[(T - T_z)^4 - \left(T_f - T_z\right)^4] \qquad (6)$$

where h_c is the convective heat transfer coefficient, taken as 25 W/(m^2 K) for ASTM E-119 and 50 W/(m^2 K) for hydrocarbon fire; T_f is the fire temperature determined from standard or hydrocarbon fire curve; T_z is the absolute zero temperature, assigned as -273 K; σ is the Stefan–Boltzmann constant, and it is equal to 5.67×10^{-8} W/(m^2 K^4); ε_m is the emissivity of the material, which is taken as 0.7 for concrete and ε_f is the emissivity of the fire. In the model, the maximum allowable temperature change per increment was specified as 100 ℃, and the maximum allowable emissivity change per increment is 0.1. The model uses a direct full Newton equation solver. Moreover, an automatic time-stepping was followed with a maximum increment size of 100s. The default convergence criteria in ABAQUS were applied, wherein the convergence threshold was set at a ratio of 0.005 between the largest residual and the corresponding average flux norm, and at a ratio of 0.01 between the largest solution correction and the largest corresponding incremental solution value.

2.5.Structural analysis

Using transient analysis, a combination of thermal, mechanical, and damage models were employed to simulate the behaviour of concrete structures under fire conditions. The nodal temperature time history was obtained from the thermal analysis. During the transient mechanical/structural analysis, the nodal temperatures were retrieved from the temperature time history for the analysis time step. The nodal temperatures were considered as thermal loads in the structural model. Non-linear implicit dynamic analysis was used in the structural analysis to compute displacements and stresses at each node of the RC wall. This type of analysis is a powerful tool for modelling the behaviour of complex structures under a wide range of loading conditions. In ABAQUS, this type of analysis involves solving complex equations that describe the mechanical behaviour of the structure over time. The equations used in non-linear implicit dynamic analysis in Abaqus can be divided into five main categories: continuity, equilibrium, constitutive, kinematic, and boundary conditions. The continuity equation expresses the conservation of mass and ensures that the mass balance is maintained throughout the simulation. The equilibrium equations express the balance of forces and moments in the structure and ensure that the structure remains in equilibrium throughout the simulation. As described in the materials section, the constitutive equations relate the stress and strain in the modelled material. The kinematic equations relate the displacement, velocity, and acceleration of the structure and ensure that the motion of the structure is consistent with the applied loads and the laws of physics. Finally, the boundary conditions specify the constraints on the structure, such as fixed supports or applied loads, and ensure that the structure is appropriately constrained and that the simulation is physically meaningful. These equations are solved numerically using an appropriate integration scheme at each time step. The solution at each time step is used to update the nodal displacements and stresses which are then used to compute the solution at the next time step. Automatic time incrementation was used in the analysis. The main factors used to control adjustments to the time increment size for an implicit dynamic procedure are the convergence behaviour of the Newton iterations and the accuracy of the time integration. Default convergence criteria in ABAQUS was used as explained in section 2.4.

2.6. Failure criteria of RC walls under fire

The failure limit states of reinforced concrete walls under fire are a critical consideration for ensuring the safety of buildings. International standards such as ISO 834, ASTM E119, and EC2 provide guidance on evaluating the fire resistance of reinforced concrete walls and establishing their performance under fire. Various factors, such as the duration and intensity of the fire and the type and thickness of the concrete wall, can impact the failure mode of reinforced concrete walls under fire. The following are failure modes with their standard limits:

- Structural failure occurs when the wall loses its load-carrying capacity due to the loss of structural strength caused by the fire. This can be caused by the thermal expansion of the concrete, which can lead to cracking and spalling, ultimately resulting in the wall's collapse. Concrete stresses are used to evaluate the wall's fire resistance for this failure state. The stresses in the concrete were monitored during the fire duration at multiple points. When the stress in concrete at a point exceeds the concrete compressive strength according to EC2 [24], failure of the wall was assumed at that point.
- Thermal failure occurs when the concrete wall's temperature wall reaches a critical point, causing a significant reduction in the mechanical properties of its construction material. Failure limit states of RC walls under fire can vary depending on the specific building design, construction, and fire protection measures in place. For this study, the fire resistance was found based on the time steel reinforcement reached a temperature of 593℃ [36].

- Based on the insulation criterion, according to ASTM 2015, failure of a wall may occur when the temperature of the unexposed surface exceeds 139℃ above its initial temperature.

The failure of the walls in the proceeding sections was checked following the limits stated above.

3. Results and Discussion

3.1. Validation of the developed FE models

Validation of the developed finite element (FE) models is a crucial step in ensuring the integrity and dependability of numerical simulations. In this study, the developed FE models were validated utilising experimental data for reinforced concrete walls exposed to fire in Mueller and Kurama [8] and Ngo et al. [5]. The experimental data were utilised to simulate the fire exposure of the walls, and the outcomes were compared with those obtained from the numerical simulation. The comparison was performed for temperature profiles (thermal response) and out-of-plane displacements (structural response).

3.1.1 Thermal response

Reinforced concrete walls were subjected to ASTM E119 curve. For each specimen, the fire curve was applied to one side of the wall (the exposed side). Nodal temperatures from the heat-transfer analysis were compared to the reported values in the experiments conducted by Ngo et al. [5] and Mueller and Kurama [8]. The temperature versus time curve was plotted for different nodes in the FE model depending on their location. Three temperature profiles were plotted for WALL1 and WALL2. Sensor 1 represents a node that is 15 mm away from the exposed surface, sensor 2 represents a node that is 30 mm away from the exposed surface in addition to a sensor that is attached to the unexposed face.

It can be deduced from Fig. 4 that the temperature-time curve obtained from the FE model for different nodes along the thickness of the wall exhibited good agreement with the experimental curve, validating the accuracy of the numerical simulation. Few discrepancies are observed, which could be due to various factors, such as uncertainties in material properties, heat transfer mechanisms, and boundary conditions. For WALL2, it can be noticed that the temperature-time curve for sensor 1 was cut at approximately 13 min. This is due to the concrete spalling of WALL2, a high-strength concrete wall, during the fire test. It resulted in a malfunction of the temperature sensor on the surface, preventing it from reading until the end of the test. Since the spalling effect is not considered in the material modelling, the temperature-time curve continues for the 2-hours fireexposure.

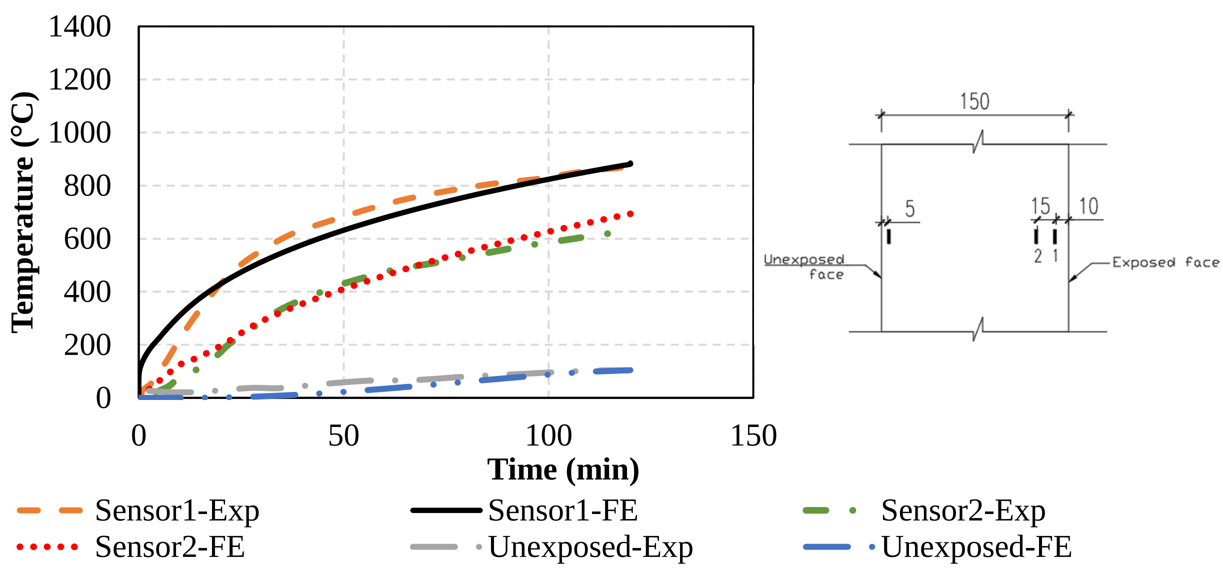

(a) WALL1

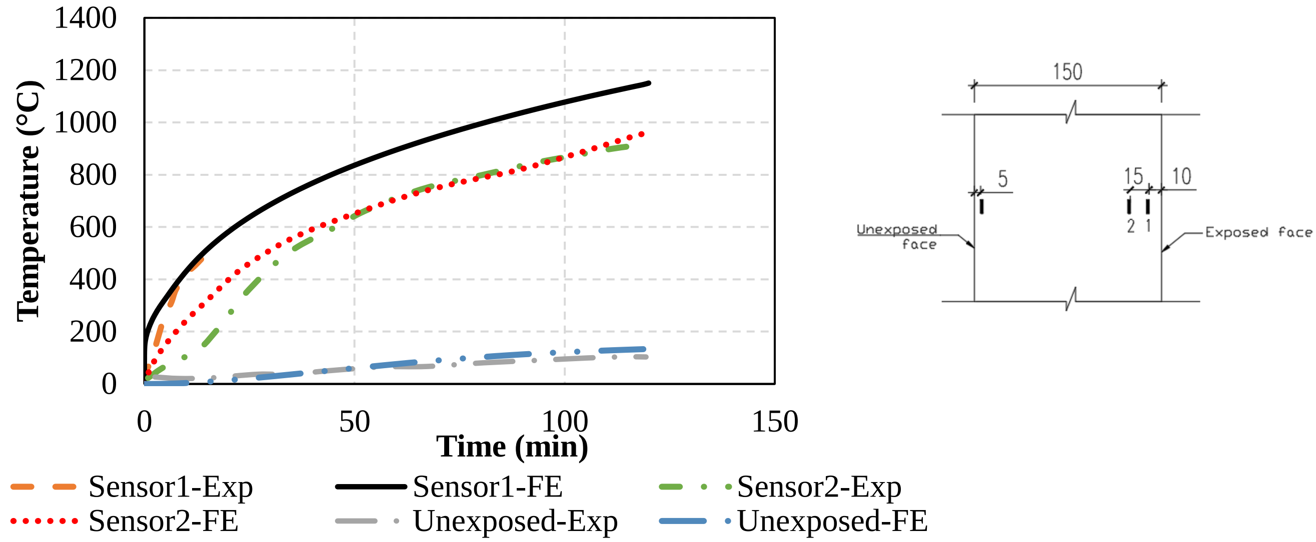

(b) WALL2

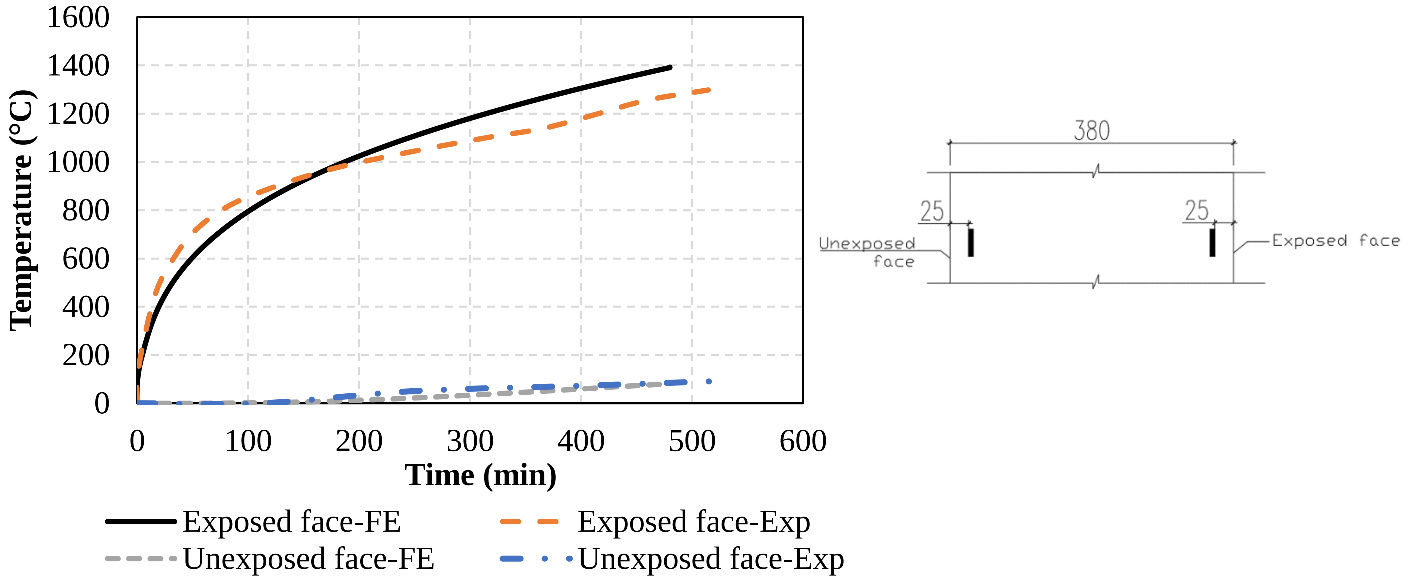

(c) WALL3

Fig. 4: Validation of the thermal response from FE model with experimental results

3.1.2 Structural response

The structural response of Reinforced Concrete (RC) walls under fire conditions was investigated using the FE model. The results were presented in terms of the out-of-plane (lateral) displacement at the midheight of the wall versus time. The structural response of the RC wall exhibited distinct behaviour in response to the ASTM E119 standard fire test. A trend can be observed in the three specimens in Fig. 5, which is characterised by a reduction in the displacement after a period of time, which is around 90 min for the first two specimens and approximately 160 min for WALL3. This reduction in displacement can be attributed to the increased thermal expansion of the exposed wall surface compared to the thermal expansion on the unexposed face, which caused the walls to bow back. Moreover, the reduction in the strength of the constituent materials at the exposed surface causes the wall to bow back towards the furnace. Bowing back towards the fire is a typical phenomenon of RC walls and can be clearly observed in specimen 3, which demonstrated the behaviour of an RC wall subjected to an 8-hour fire. The numerical model accurately captured these distinct structural responses of the RC wall under fire conditions, validating the accuracy of the simulation.

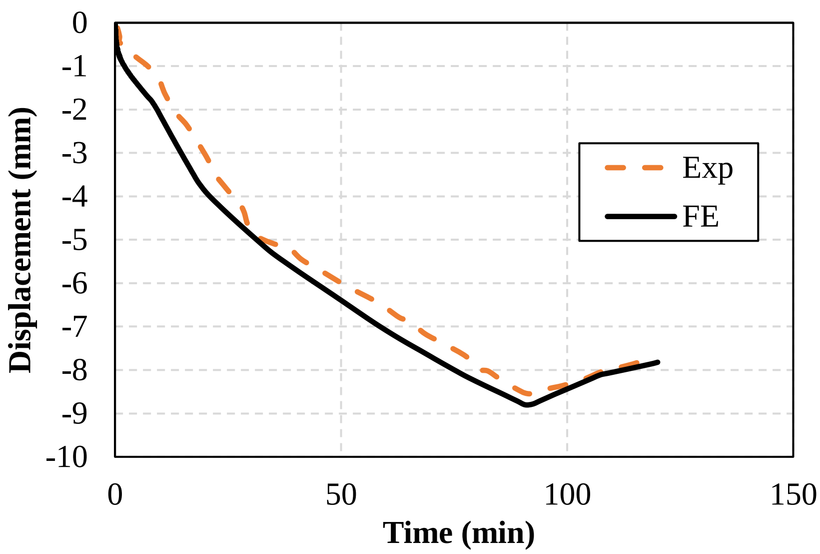

(a) WALL1

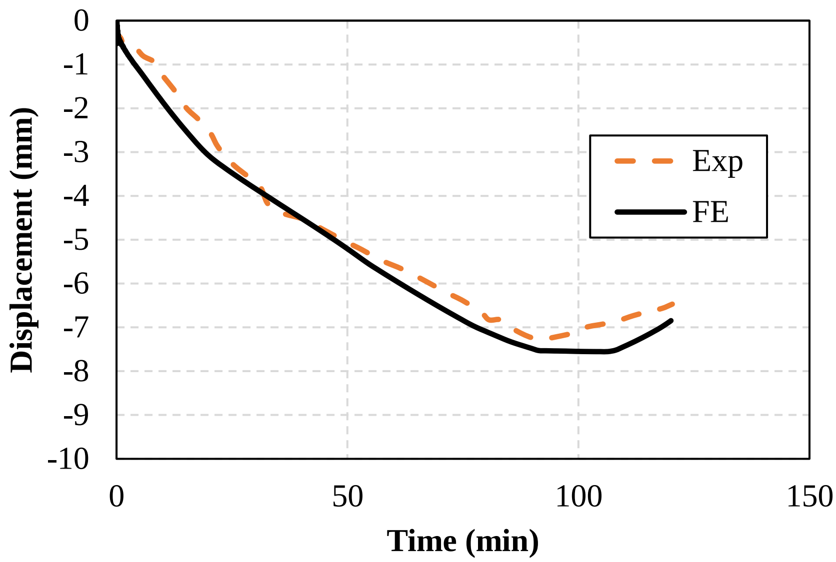

(b) WALL2

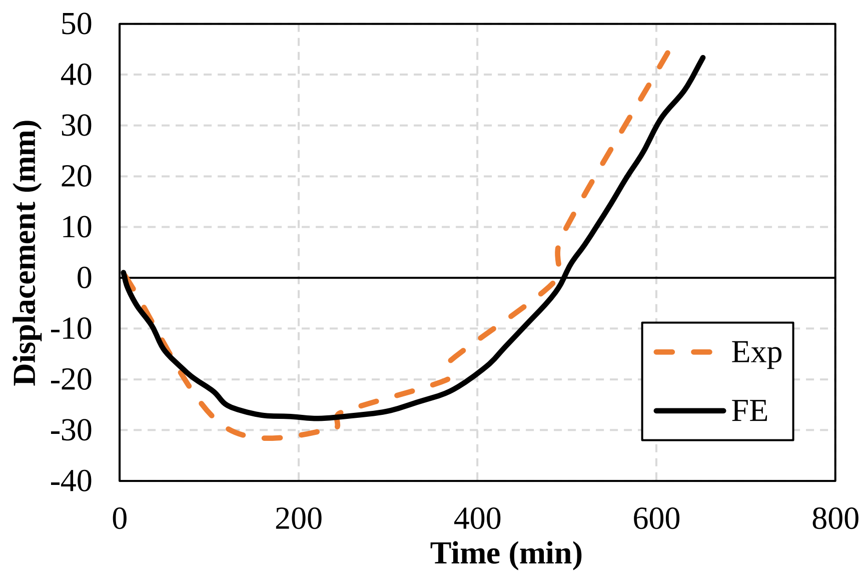

(c) WALL3

Fig. 5: Validation of the structural response from FE model with experimental results

4. Parametric Study

Various factors can influence the structural response of RC walls under fire conditions. Therefore, carefully considering these factors is essential for accurately assessing and designing fire-resistant RC walls. A parametric study was conducted to evaluate the effect of various factors on the response of RC walls to fire, including the fire scenario, concrete cover, reinforcement, and wall thickness. The fire resistance of the wall was measured following the previously mentioned failure criteria. The fire resistance was also compared to existing design guidelines, namely, EC2 [32] and ASCE manual of practice [37].

4.1. Fire Scenario

Understanding the effects of different fire scenarios on the behaviour of RC walls is essential for improving the safety and resilience of buildings in the face of fire hazards. Fire scenarios, such as ASTM E119 and hydrocarbon fires, can affect RC walls' structural performance and safety. ASTM E119 is a standard test method used to evaluate the fire resistance of various building elements, including walls. During this test, a fire is applied to one side of the wall to achieve specified temperatures throughout a specified time. RC walls subjected to ASTM E119 may experience cracking, spalling, and loss of strength but can still maintain their structural integrity and prevent the spread of fire to other parts of the building. On the other hand, hydrocarbon fires can result in more severe effects on RC walls due to the higher temperatures and faster heat transfer rates. The intense heat can cause the concrete to rapidly lose strength and undergo significant spalling, leading to a possible wall collapse. This study investigated impact of ASTM E119 and hydrocarbon fire scenarios on normal-strength and high-strength concrete walls. The dimensions of the tested wall are the same as specimen WALL1 (2400×1000×150). The discussed failure criteria were followed to identify the failure mode of RC walls. In the four investigated cases, the local damage governed the failure mode, i.e. concrete reaching the designated compressive strength by EC2. Therefore, the reduction in compressive strength following EC2 was plotted against the time corresponding to the specified temperature. Moreover, the maximum compressive stress in concrete elements was plotted against time. This was conducted by mapping temperatures obtained from the thermal model with stresses obtained from the structural model with respect to time. From Figs. 6-7, it can be noticed that the fire resistance dropped from 100 to 42 min for normal-strength concrete wall, and from 88 to 29 min for high-strength concrete wall. Although the predicted fire resistance according to EC2 for a wall thickness of 150 mm is 2 hours, neither the normal- nor high-strength concrete wall reached 120 min under the standard fire nor the hydrocarbon fire. Moreover, the fire resistance of the wall under hydrocarbon fire was highly compromised. These findings highlight the significant impact of fire scenarios and their heating rates on fire performance.

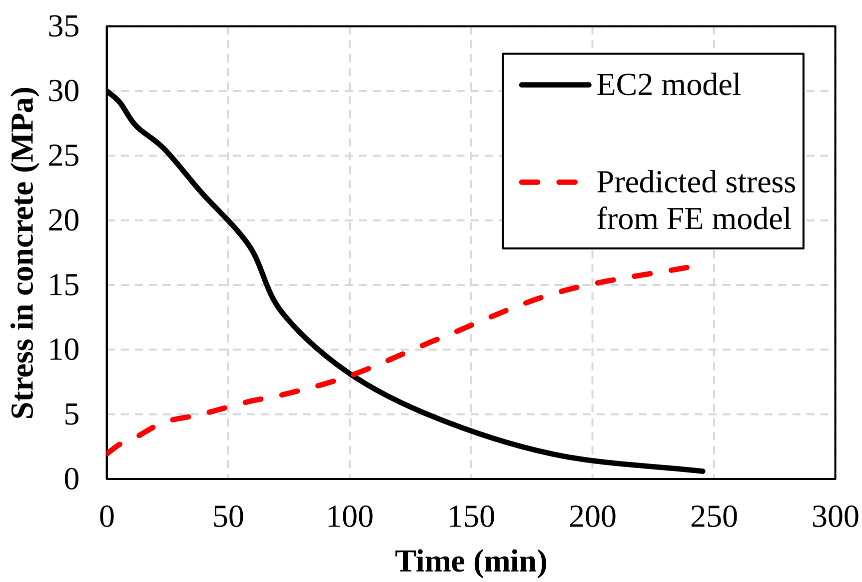

Fire Resistance= 100 min

(a) Under ASTM-E119 fire

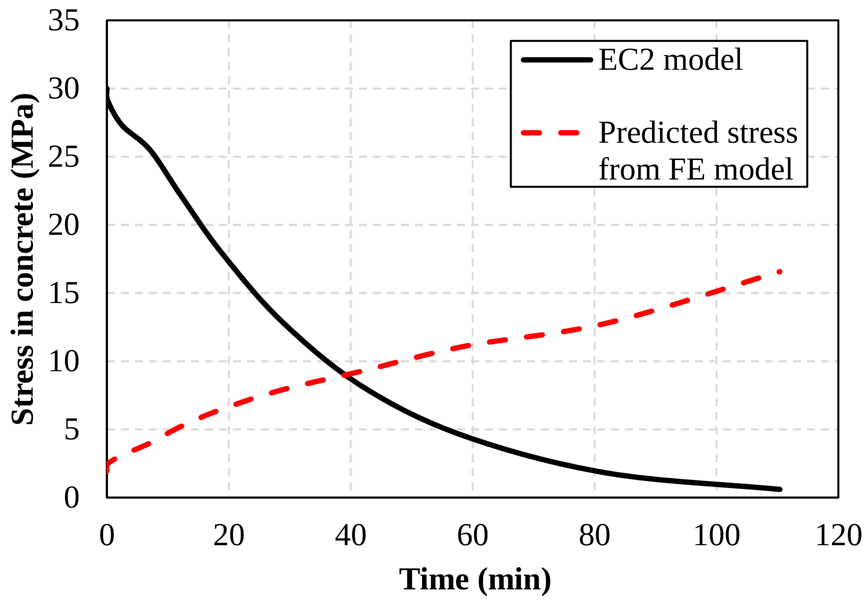

Fire Resistance= 42 min

(b) Under hydrocarbon fire curve

Fig. 6: Maximum stresses in normal-strength concrete wall

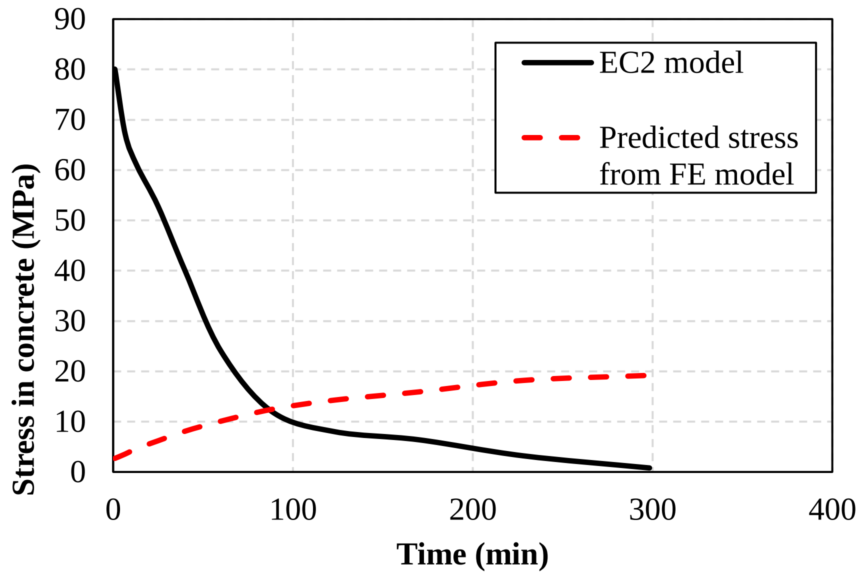

Fire Resistance= 88min

(a) Under ASTM-E119 fire

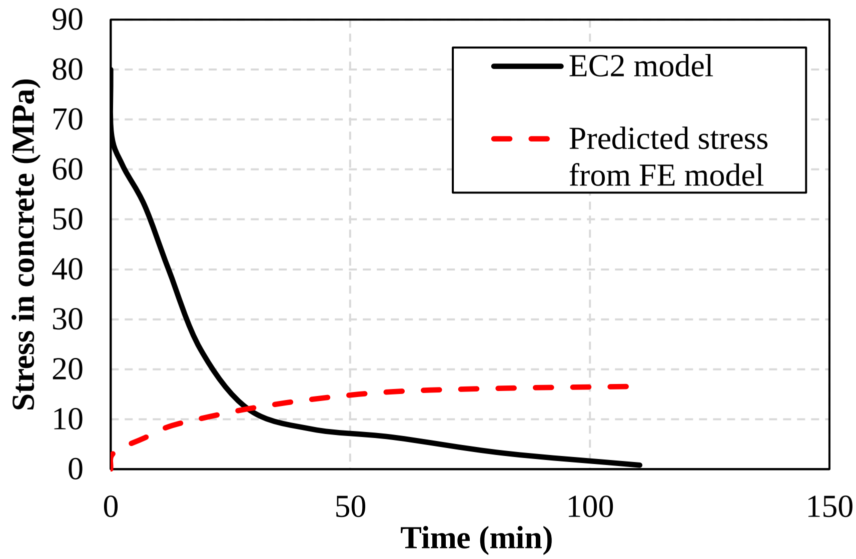

Fire Resistance= 29min

(b) Under hydrocarbon fire curve

Fig. 7: Maximum stresses in high-strength concrete wall

4.2. Concrete cover

Concrete cover significantly affects the fire resistance of reinforced concrete (RC) walls, as it acts as a protective layer, preventing the steel bars from being exposed to high temperatures during a fire, thus maintaining the wall's structural ability to sustain loading. It is essential to ensure that the concrete cover for RC walls is designed and constructed appropriately, considering the expected fire exposure and the desired fire resistance time. This is particularly important in buildings at higher risk of fire, such as those that store or handle flammable materials. The minimum concrete cover in RC walls is specified by various design codes and standards, such as the American Concrete Institute (ACI-318) Building Code Requirements for Structural Concrete [38] and ACI-216.1.14 (Code Requirements for Determining Fire Resistance of Concrete and Masonry Construction Assemblies) [39]. According to ACI-318, the minimum concrete cover for

RC walls is usually in the range of 25-40 mm (1-1.5 inches) for mild exposure conditions and can be higher for more severe exposure conditions. On the other hand, ACI-216 does not specify a minimum concrete cover for RC walls. However, it states that the minimum concrete cover reinforcement in RC columns should not be less than 25 mm (1 in.) times the required fire resistance hours, or 50 mm (2 in.), whichever is less. In ASCE Manuals and Reports on Engineering Practice No. 78 [37], the minimum concrete cover is only mentioned for RC columns, which equals the fire resistance or 50 mm, whichever is less, for a required fire resistance of less than 3 hours. For fire resistances that are more than 3 hours: the minimum concrete cover is ½ (R-3)+2, where R is the desired fire resistance.

In this study, three values of the concrete cover were investigated for a normal-strength concrete wall with a thickness of 150 mm under standard ASTM-E119 and hydrocarbon fire curves. The values are: 25, 50, and 64 mm, corresponding to a designated fire resistance of 2, 3, and 4 hours according to ASCE manuals No. 78 [37]. Fig. 8 plots the fire resistance against concrete cover considering ASTM-E119 standard fire, hydrocarbon fire curve, and ASCE manuals No. 78 predictions. It can be seen that the ASCE predictions were conservative. The obtained fire resistance from the FE model was higher than the predicted one for concrete covers 25, and 50 mm, respectively. For the concrete cover of 64 mm, the ASCE-predicted fire resistance was less than the model-predicted value in the case of ASTM-E119 fire and longer in the case of the hydrocarbon fire. However, the percentage differences were only 2% and 4%, respectively. Thus, it can be concluded that the existing codes provide conservative estimations of the fire resistance of RC walls for their recommended reinforcement concrete cover.

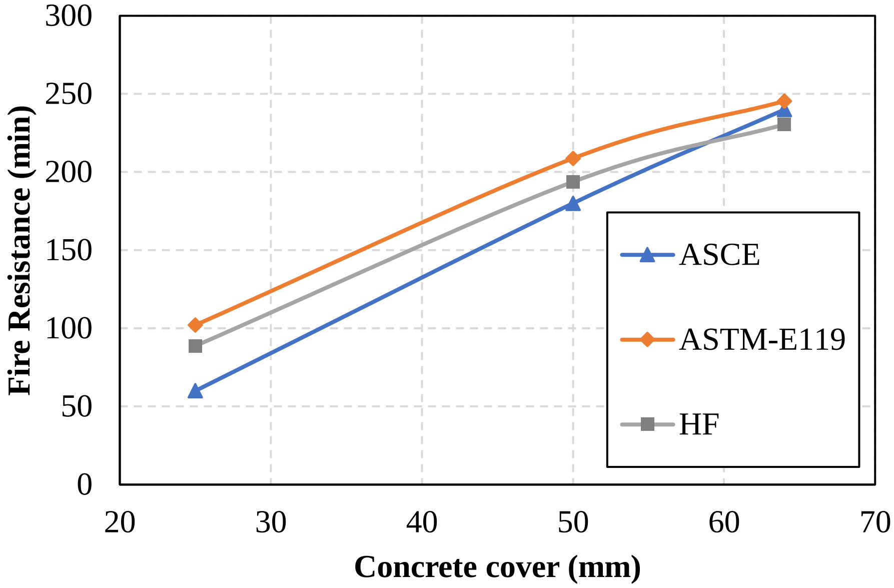

Fig. 8: Effect of concrete cover on the fire resistance of RC walls

4.3. Reinforcement

This section investigates the reinforcement ratio and configuration effect on RC walls' behaviour under standard fire. Regarding the reinforcement ratio, three values were tested. The first corresponds to the minimum reinforcement ratio of RC walls specified by ACI-318 [38], which is 0.12%. The second reinforcement ratio is a typical value generally used in common practice, which is 1.2%. This value was doubled, and the effect of doubling the reinforcement ratio on the structural response under fire was explored. Furthermore, the placement of reinforcement in one mat or two mats was also examined since ACI-318 permits such placement for walls.The reinforcement ratio of one mat wall was 1.2%. From Fig. 9, it can be seen that the reinforcement ratios affect the out-of-plane displacement. However, the percentage difference between the maximum displacement corresponding to the minimum reinforcement and the maximum displacement of the wall having a 1.2% reinforcement ratio is only 9%. Doubling the reinforcement ratio to 2.4% did not affect the maximum out-of-plane displacement but delayed the change in the wall's displacement direction from 92 min. to 107 min. Having one reinforcement mat in the middle of the wall with the same reinforcement ratio did not influence the magnitude of the out-of-plane displacement, Fig. 9. Nevertheless, the wall with one mat experienced a clear double curvature at 5.75 hours as shown in Fig. 10(a). At this point, all steel bars were under compression. Examining the contour plot of the wall with double mats, the wall bowed at the side of the fire (towards the furnace), and all steel bars were under tension (single curvature at 5.75). This wall then started to have a double curvature behaviour at about 7 hours, Fig. 10(c). However, all steel bars remained under tension for the whole period of fire exposure (8 hours), Fig. 10(c). Therefore, it can be deduced that the reinforcement had a relatively minor effect on the deformation value. Nevertheless, it had a noticeable influence on the deformation pattern. The double mat wall will generally have a single curvature when exposed to fire for long durations. Moreover, doubling the reinforcement ratio in the wall resulted in a shift in the displacement snap point.

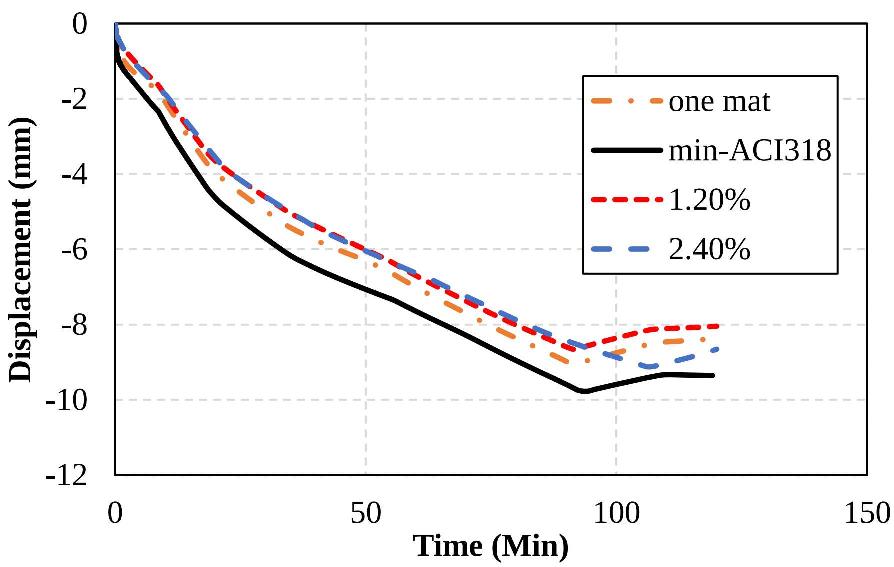

Fig. 9: Out-of-plane displacement for different reinforcement ratios and configuration

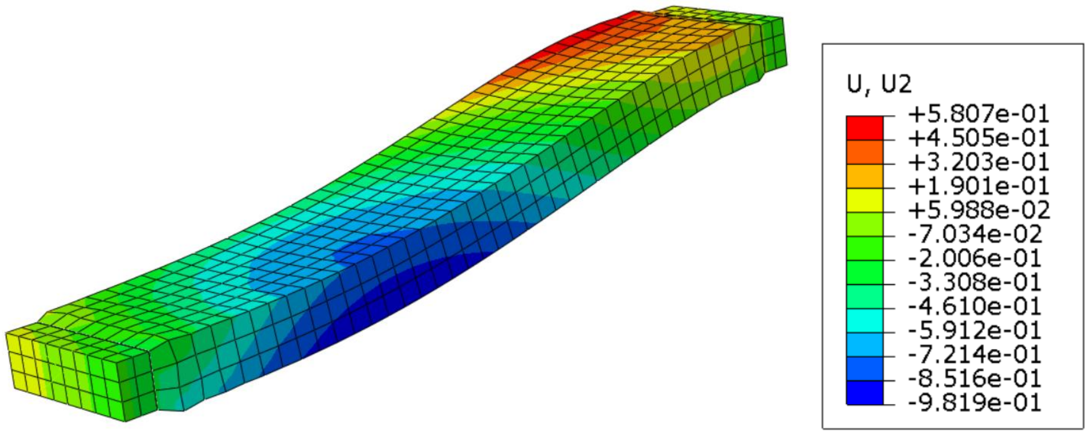

(a) U2 for a wall with one mat in the middle at 5.75^{th} hrs

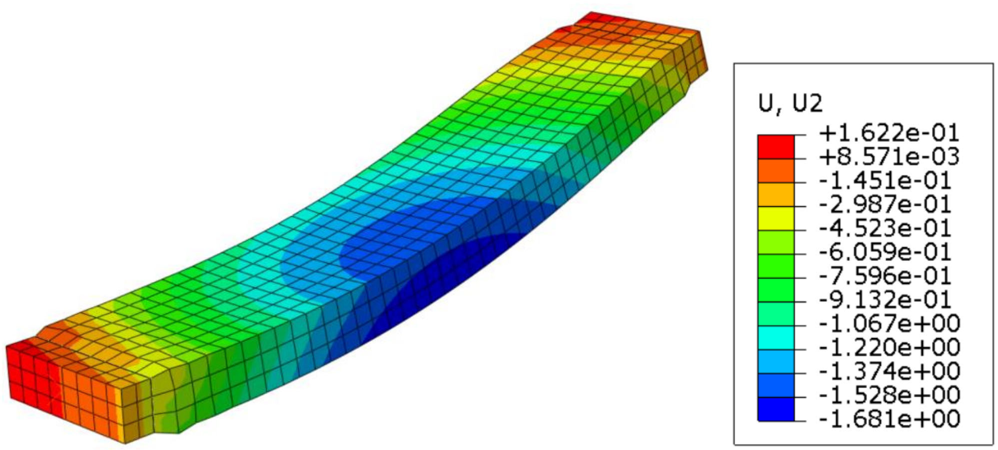

(b) U2 for a wall with two reinforcement mats at 5.75^{th} hrs

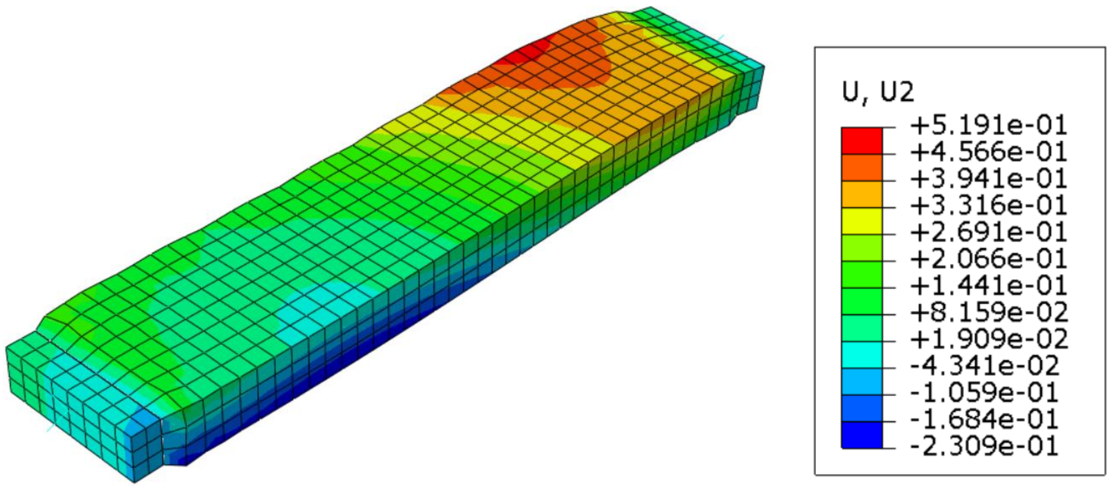

(c) U2 for a wall with two reinforcement mats at 7th hrs

Fig. 10: Contour plot for the lateral displacement of investigated walls

4.4. Wall Thickness

The effect of wall thickness on the behaviour of RC walls was investigated in this study. A series of finite element simulations were performed on different wall thickness values under standard and hydrocarbon fire tests. EC2 [32] specifies a minimum wall thickness corresponding to a desired fire resistance value as presented in Table 2. It should be noted that the minimum wall thickness depends on the fire exposure and the degree of utilisation in the fire situation (μ_{fi}) according to EC2. This ratio is calculated by dividing the axial load in the fire situation by the design resistance at normal temperature conditions, the values ranged from 0.1 to 0.2 for the tested walls. The analysis results were presented in terms of the out-of-plane displacement, concrete stresses, and the corresponding fire resistance. The fire resistance values were compared to those provided by EC2. It was noticed that walls, which have a thickness of less than 120 mm experienced a deformation away from the fire/furnace for the whole exposure period as can be seen in Fig. 11 and Fig. 12. On the other hand, the analysis of the walls with a thickness of 120 mm or more showed that the wall bows toward the furnace and reverse bowing occurs, very similar to previous results in Mueller and Kurama [8], Ngo. et al. [5], and Kumar and Kodur [11]. The values of the fire resistance obtained from the FE model for each wall, determined by local concrete crushing, are compared to the designated values from EC2 for the standard and hydrocarbon fire scenarios. The comparison is illustrated in Fig. 13. It can be seen that EC2 overestimated the fire resistance values of the walls, indicating that the specified thicknesses are not adequate to provide the desired fire rates under either fire scenario. In fact, the difference in the fire resistance was more pronounced in the case of hydrocarbon fire, indicating the importance of considering the effect of fire types when designing facilities subjected to critical fire scenarios.

Table 2: Minimum wall thickness corresponding to required fire resistance in accordance with EC2 [32]

Standard fire resistance (min)	***Wall thickness (mm)***
30	100
60	110
90	120
120	150
240	230

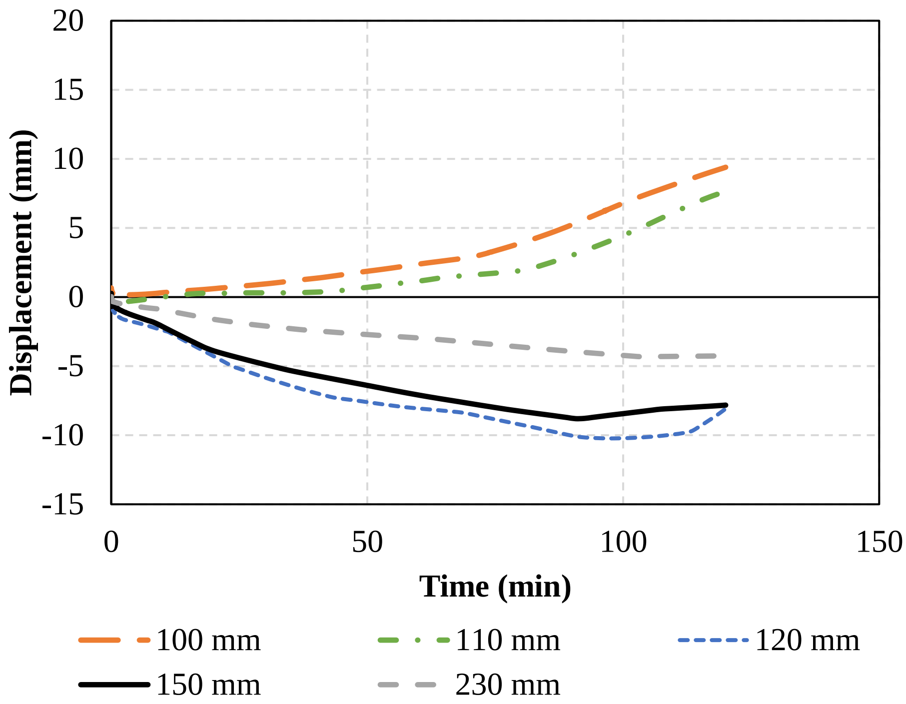

Fig. 11: Effect of wall thickness on the out-of-plane displacement of the wall under standard fire

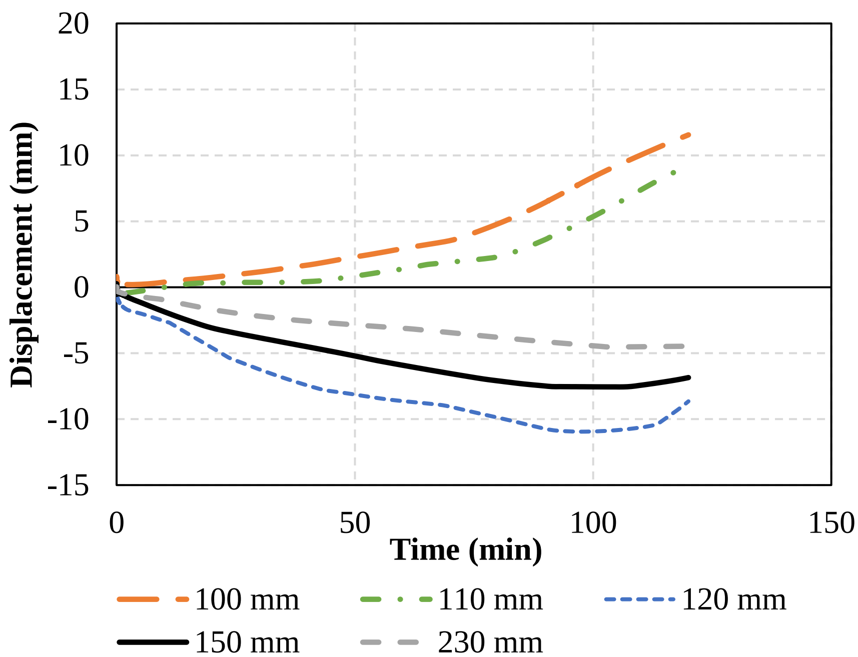

Fig. 12: Effect of wall thickness on the out-of-plane displacement of the wall under hydrocarbon fire

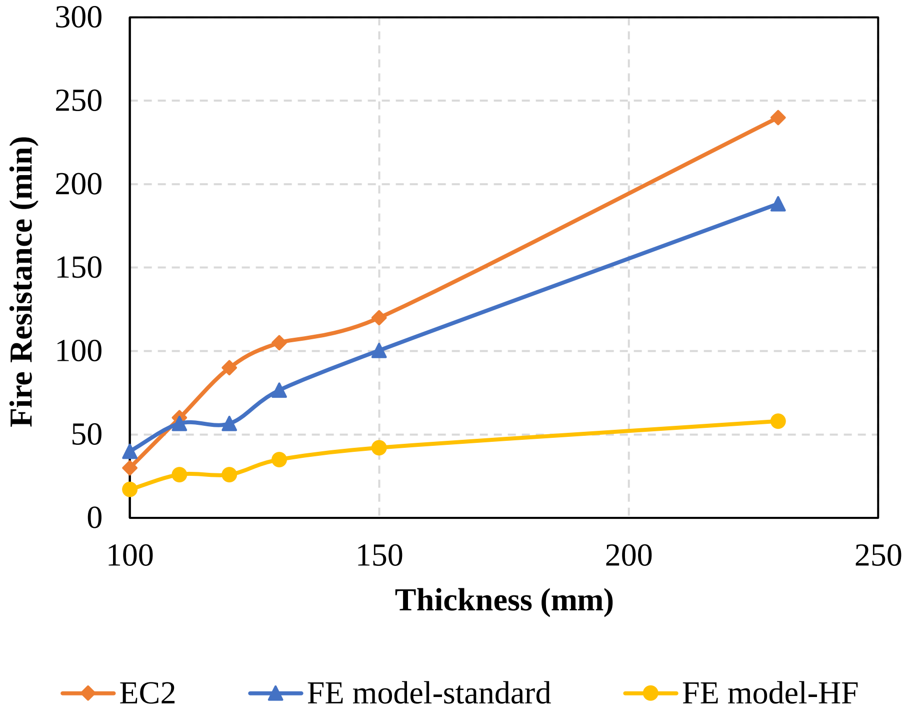

Fig. 13: Comparison of the fire resistance obtained from the FE model with EC2

5. Summary and Conclusions

This study presents the results of a 3-D FE numerical investigation of the thermal and structural behaviour of reinforced concrete (RC) walls under fire exposure. A total of 17 FE models were developed to inspect the influence of different parameters on the response of RC walls. The developed model accounts for thermal and mechanical material properties and non-linearities. The walls were subjected to standard ASTM-E119 and hydrocarbon fire scenarios, and their thermal and structural behaviour were examined. Three models were validated and compared with published experimental data. Factors affecting the performance of RC walls were inspected by conducting a parametric study that tested the effect of the fire scenario, concrete cover, reinforcement ratio and configuration, and wall thickness. The results were compared with design guidelines in the existing codes of practice. The following findings were deducted from this study:

- The FE model could accurately simulate the behaviour of RC walls under fire, and the results obtained from the FE model were in good agreement with the experimental data. The temperature profiles obtained from the FE model were similar to those observed during the experiments, indicating that the model could capture the thermal behaviour of the walls accurately. Moreover, the FE model was also able to predict the out-of-plane displacement of the RC walls, which is an important measure of the structural performance of the walls. The good correlation between the FE model and the experimental data suggests that the model can be a reliable tool for predicting the structural behaviour of RC walls under fire.
- The fire resistance of the examined walls was highly compromised under hydrocarbon fire. The predicted fire resistance from the FE model was lower than the value provided by EC2.
- Regarding the reinforcement concrete cover, the predictions of ASCE manual of practice provide conservative estimations of the fire resistance of RC walls corresponding to specified concrete cover values under standard and hydrocarbon fire scenarios.
- The minimum wall thickness specified by EC2 may not be sufficient to achieve the desired fire resistance, indicating a need for further investigation and potential revision of the current standards.
- Doubling the reinforcement ratio or having one reinforcement mat in the middle of the wall does not significantly impact the maximum out-of-plane displacement but can

affect the curvature behaviour of the wall. These findings can be useful for optimising the design of reinforced concrete walls to improve their performance under fire conditions.

- Further research and validation studies are warranted to enhance the understanding of the structural response of RC walls under fire conditions and to ensure the safety of buildings and occupants.

References

[1] D. A. C. and J. G. Sanjayan, "Tests of Load-Bearing Slender Reinforced Concrete Walls in Fire," *ACI Struct J*, vol. 97, no. 2, doi: 10.14359/853.

[2] K. A. Mueller and Y. C. Kurama, "Out-of-plane behaviour and stability of five planar reinforced concrete bearing wall specimens under fire," *ACI Struct J*, vol. 112, no. 6, pp. 701–712, Nov. 2015, doi: 10.14359/51687908.

[3] I. Almeshal, B. H. Abu Bakar, and B. A. Tayeh, "Behaviour of Reinforced Concrete Walls Under Fire: A Review," *Fire Technology*, vol. 58, no. 5. Springer, pp. 2589–2639, Sep. 01, 2022. doi: 10.1007/s10694-022-01240-3.

[4] W.C. Hayhoe, M.A. Youssef, "Structural Behaviour of Concrete Walls during or after Exposure to Fire: A Review", in Proceedings of the CSCE 2013 General Conference, Montréal, Québec, May 2013.

[5] T. Ngo, S. Fragomeni, P. Mendis, and B. Ta, "Testing of normal-and high-strength concrete walls subjected to both standard and hydrocarbon fires," *ACI Struct J*, vol. 110, no. 3, pp. 503–510, May 2013, doi: 10.14359/51685607.

[6] Y. Q. Zheng and J. P. Zhuang, "Analysis on Fire Resistance of Reinforced Concrete Wall," *Adv Mat Res*, vol. 243–249, pp. 797–800, 2011, doi: 10.4028/www.scientific.net/AMR.243-249.797.

[7] J. Chen, E. Hamed, and R. Ian Gilbert, "Structural Performance of Reinforced Concrete Walls under Fire Conditions," *Journal of Structural Engineering*, vol. 146, no. 3, Mar. 2020, doi: 10.1061/(asce)st.1943-541x.0002519.

[8] K. A. Mueller, Y. C. Kurama, and M. J. McGinnis, "Out-of-plane behaviour of two reinforced concrete bearing walls under fire: A full-scale experimental investigation," *ACI Struct J*, vol. 111, no. 5, pp. 1101–1110, 2014, doi: 10.14359/51686814.

[9] K. A. Mueller and Y. C. Kurama, "Out-of-plane behaviour and stability of five planar reinforced concrete bearing wall specimens under fire," *ACI Struct J*, vol. 112, no. 6, pp. 701–712, Nov. 2015, doi: 10.14359/51687908.

[10] K. A. Mueller and Y. C. Kurama, "Out-of-plane behaviour of reinforced concrete bearing walls after one-sided fire," *ACI Struct J*, vol. 114, no. 1, pp. 149–160, Jan. 2017, doi: 10.14359/51689445.

[11] P. Kumar and V. K. R. Kodur, "Modelling the behaviour of load bearing concrete walls under fire exposure," *Constr Build Mater*, vol. 154, pp. 993–1003, Nov. 2017, doi: 10.1016/j.conbuildmat.2017.08.010.

[12] G. Karaki, R. Hawileh, and V. Kodur, "Probabilistic-Based Approach for Evaluating the Thermal Response of Concrete Slabs under Fire Loading,"

Journal of Structural Engineering, vol. 147, Apr. 2021, doi: 10.1061/(ASCE)ST.1943-541X.0003039.

[13] M. Z. Naser, R. A. Hawileh, and H. A. Rasheed, "Performance of RC T-beams externally strengthened with CFRP laminates under elevated temperatures," *Journal of Structural Fire Engineering*, vol. 5, no. 1, pp. 1–24, Mar. 2014, doi: 10.1260/2040-2317.5.1.1.

[14] R. A. Hawileh, M. Naser, W. Zaidan, and H. A. Rasheed, "Modelling of insulated CFRP-strengthened reinforced concrete T-beam exposed to fire," *Eng Struct*, vol. 31, no. 12, pp. 3072–3079, Dec. 2009, doi: 10.1016/j.engstruct.2009.08.008.

[15] G. Karaki and M. Z. Naser, "An approach for developing probabilistic models for temperature-dependent properties of construction materials from fire tests and small data," *Fire Mater*, 2022, doi: 10.1002/fam.3116.

[16] M. Assad, R. A. Hawileh, and J. A. Abdalla, "Modelling the behaviour of CFRP-strengthened RC slabs under fire exposure," *Procedia Structural Integrity*, vol. 42, pp. 1668–1675, 2022, doi: 10.1016/j.prostr.2022.12.210.

[17] H. Hostetter, M. Z. Naser, R. A. Hawileh, G. Karaki, and H. Zhou, "Enhancing fire resistance of reinforced concrete beams through sacrificial reinforcement," *Architecture, Structures and Construction*, vol. 2, no. 2, pp. 311–322, Jul. 2022, doi: 10.1007/s44150-022-00061-w.

[18] A. Daware, M. Z. Naser, and G. Karaki, "Generalised temperature-dependent material models for compressive strength of masonry using fire tests,

statistical methods and artificial intelligence," *Architecture, Structures and Construction*, vol. 2, no. 2, pp. 223–229, Jul. 2022, doi: 10.1007/s44150-021-00019-4.

[19] R. A. Hawileh and V. K. R. Kodur, "Performance of reinforced concrete slabs under hydrocarbon fire exposure," *Tunnelling and Underground Space Technology*, vol. 77, pp. 177–187, Jul. 2018, doi: 10.1016/j.tust.2018.03.024.

[20] K. A. Mueller and Y. C. Kurama, "Numerical modelling of three reinforced concrete bearing wall tests subject to one-sided standard fire," *ACI Structural Journal*, vol. 116, no. 5. American Concrete Institute, pp. 29–41, 2019. doi: 10.14359/51716756.

[21] S. Ni and T. Gernay, "Considerations on computational modelling of concrete structures in fire," *Fire Saf J*, vol. 120, Mar. 2021, doi: 10.1016/j.firesaf.2020.103065.

[22] E. Ryu, H. Kim, Y. Chun, I. Yeo, and Y. Shin, "Effect of heated areas on thermal response and structural behaviour of reinforced concrete walls exposed to fire," *Eng Struct*, vol. 207, Mar. 2020, doi: 10.1016/j.engstruct.2020.110165.

[23] J. Y. Kang, H. A. Yoon, E. M. Ryu, and Y. S. Shin, "Analytical studies for the effect of thickness and axial load on load bearing capacity of fire damaged concrete walls with different sizes," *Journal of Structural Integrity and Maintenance*, vol. 4, no. 2, pp. 58–64, Apr. 2019, doi: 10.1080/24705314.2019.1603189.

[24] S. Lee and C. Lee, "Fire resistance of reinforced concrete bearing walls subjected to all-sided fire exposure," *Materials and Structures/Materiaux et Constructions*, vol. 46, no. 6, pp. 943–957, Jun. 2013, doi: 10.1617/s11527-012-9945-8.

[25] T. Morita, H. Yamashita, M. Beppu, and M. Suzuki, "A Study on Structural Behaviour of Reinforced Concrete Walls Exposed to Hydrocarbon Fire Under Vertical Load," in *Fire Science and Technology 2015*, Springer Singapore, 2017, pp. 299–308. doi: 10.1007/978-981-10-0376-9_30.

[26] P. Bamonte *et al.*, "On the structural behaviour of reinforced concrete walls exposed to fire," in *Key Engineering Materials*, Trans Tech Publications Ltd, 2016, pp. 580–587. doi: 10.4028/www.scientific.net/KEM.711.580.

[27] M. Assad, R. A. Hawileh, J. A. Abdalla, and F. Abed, "Heat Transfer Analysis of Reinforced Concrete Walls in ANSYS and ABAQUS: A Comparative Study," in *2022 Advances in Science and Engineering Technology International Conferences, ASET 2022*, Institute of Electrical and Electronics Engineers Inc., 2022. doi: 10.1109/ASET53988.2022.9735001.

[28] J. Chen, E. Hamed, and R. Ian Gilbert, "Structural Performance of Reinforced Concrete Walls under Fire Conditions," *Journal of Structural Engineering*, vol. 146, no. 3, Mar. 2020, doi: 10.1061/(asce)st.1943-541x.0002519.

[29] ANSYS – Release Version 19.2, 0000. A Finite Element Computer Software and User Manual for Nonlinear Structural Analysis, ANSYS 2019, Inc. Canonsburg, PA..

[30] ASTM A370-18, 'Standard Test Methods and Definitions for Mechanical Testing of Steel Products,' ASTM International, West Conshohocken, PA, 2018.

[31] ABAQUS. ABAQUS standard user's manual. Version 19, vol. I–III. Pawtucket (America): Hibbitt, Karlsson & Sorensen, Inc.; 2019.

[32] EN 1992-1-2: Eurocode 2: Design of concrete structures - Part 1-2: General rules - Structural fire design, 1992.

[33] M. Z. Naser, "Properties and material models for modern construction materials at elevated temperatures," *Comput Mater Sci*, vol. 160, pp. 16–29, Apr. 2019, doi: 10.1016/j.commatsci.2018.12.055.

[34] K. D. Charles and P. Robert, "Flexural Members with Confined Concrete," *Journal of the Structural Division*, vol. 97, no. 7, pp. 1969–1990, Jul. 1971, doi: 10.1061/JSDEAG.0002957.

[35] M. Hafezolghorani, F. Hejazi, R. Vaghei, M. S. Bin Jaafar, and K. Karimzade, "Simplified damage plasticity model for concrete," in *Structural Engineering International*, Int. Assoc. for Bridge and Structural Eng. Eth-Honggerberg, Feb. 2017, pp. 68–78. doi: 10.2749/101686616X1081.

[36] T. T. Lie, *Structural Fire Protection: Manual of Practice.* American Society of Civil Engineers, 1992.

[37] Building Code Requirements for Structural Concrete (ACI 318-14) Commentary on Building Code Requirements for Structural Concrete (ACI 318R-14) An ACI Standard and Report from IHS, 2014.

[38] Joint ACI/TMS Committee 216. and Masonry Society (U.S.), *Code requirements for determining fire resistance of concrete and masonry construction assemblies: an ACI/TMS Standard*.